Preventive Power Outage Estimation Based on A Novel Scenario Clustering Strategy

Preprint

Xiaofei Wang,[1] Weijia Liu,[1] Fei Ding,[1] Yiyun Yao,[1] and Junbo Zhao[2]

1 National Renewable Energy Laboratory
2 University of Connecticut

Presented at the 2024 IEEE Power and Energy Society General Meeting
Seattle, Washington
July 21–25, 2024

NREL is a national laboratory of the U.S. Department of Energy
Office of Energy Efficiency & Renewable Energy
Operated by the Alliance for Sustainable Energy, LLC

This report is available at no cost from the National Renewable Energy Laboratory (NREL) at www.nrel.gov/publications.

Contract No. DE-AC36-08GO28308

Conference Paper
NREL/CP-5D00-87960
July 2024

Preventive Power Outage Estimation Based on A Novel Scenario Clustering Strategy

Preprint

Xiaofei Wang,[1] Weijia Liu,[1] Fei Ding,[1] Yiyun Yao,[1] and Junbo Zhao[2]

1 National Renewable Energy Laboratory
2 University of Connecticut

Suggested Citation
Wang, Xiaofei, Weijia Liu, Fei Ding, Yiyun Yao, and Junbo Zhao. 2024. *Preventive Power Outage Estimation Based on A Novel Scenario Clustering Strategy: Preprint*. Golden, CO: National Renewable Energy Laboratory. NREL/CP-5D00-87960. https://www.nrel.gov/docs/fy24osti/87960.pdf.

NREL is a national laboratory of the U.S. Department of Energy
Office of Energy Efficiency & Renewable Energy
Operated by the Alliance for Sustainable Energy, LLC

This report is available at no cost from the National Renewable Energy Laboratory (NREL) at www.nrel.gov/publications.

Contract No. DE-AC36-08GO28308

Conference Paper
NREL/CP-5D00-87960
July 2024

National Renewable Energy Laboratory
15013 Denver West Parkway
Golden, CO 80401
303-275-3000 • www.nrel.gov

NOTICE

This work was authored in part by the National Renewable Energy Laboratory, operated by Alliance for Sustainable Energy, LLC, for the U.S. Department of Energy (DOE) under Contract No. DE-AC36-08GO28308. Funding provided by U.S. Department of Energy Office of Energy Efficiency and Renewable Energy Solar Energy Technologies Office Award Number DE-EE0010422. The views expressed herein do not necessarily represent the views of the DOE or the U.S. Government.

Preventive Power Outage Estimation Based on A Novel Scenario Clustering Strategy

Xiaofei Wang, Weijia Liu, Fei Ding, Yiyun Yao
Power System Engineering Center
National Renewable Energy Laboratory
Golden, U.S.A
{xiaofei.wang, weijia.liu, fei.ding, yiyun.yao}@nrel.gov

Junbo Zhao
Department of Electrical and Computer Engineering
University of Connecticut
Storrs, U.S.A
junbo@uconn.edu

***Abstract*—The increasing occurrence of extreme weather events is challenging power grid operation. For extreme weather events, the system operator is responsible for estimating the power outages and scheduling the restoration resources. This paper proposes an outage evaluation framework to identify the possible unserved load profiles, vulnerable areas, and mobile energy adequacy. The outputs of an outage prediction model tool are used to generate numerous faulted line scenarios. Next, each scenario's nodal unserved load profile is obtained by solving a three-phase restoration model that considers repair crews and mobile energy resources (MERs). Then, a novel scenario clustering strategy is developed to cluster the unserved load profiles into multiple representative profiles which the system operator can focus on. Finally, case studies on a distribution system evaluate the damage caused by an extreme weather event and verify the effectiveness of the proposed scenario clustering strategy.**

***Index Terms*—Mobile energy resources (MERs), preventive outage evaluation, power system resilience, scenario clustering.**

I. Introduction

Resilience is a system's ability to anticipate, resist, adapt to, and timely recover from disruptions [1]. In recent decades, the number of disaster events and the corresponding economic loss have continued to increase [2]. Distribution systems, located at edges of power systems, play a critical role in restoring system after outages.

Protecting the system against extreme weather events can be divided into three stages: outage prediction based on weather forecasts, preventive resource allocation, and post-disaster recovery. Single stages and combinations of these stages have been widely studied to improve power system resilience in recent years.

The key point of outage prediction is to accurately map weather predictions to distribution system outage predictions. Statistical model-based and machine learning (ML) methods are commonly used for the mapping. In [3], the line fault probability was fitted based on historical data, and Monte Carlo Simulation was used to generate sufficient faulted line scenarios. ML approaches, such as Bayesian decision theory [4], and decision tree and ensemble boosted tree [5], were used to predict outages, respectively. The commonality in ML-based methods is that the training model integrates all weather forecasts, environmental characteristics, and grid properties.

Based on outage predictions, the system operator can arrange repair crews (RCs) and prepare the necessary tools in advance. Given the available mobile energy resources (MERs) in the system, such as mobile battery energy storage systems (MBESSs) and mobile diesel generators (MDGs), the system operator can also optimally schedule these resources to minimize the unserved load. In [6][7], RCs and network reconfiguration were co-optimized for system resilience. References [8] integrated MERs into the restoration model. The commonality between these studies is that integer variables were introduced to model the transportation process of mobile resources, and thus the final mathematical model was formulated as a mixed-integer programming problem. The technical difference focused on modeling the transportation system. In [6], the traveling time between different nodes was considered constant due to the small scale of the distribution system, whereas in [8], the traveling time between nodes was considered to be different, and the travel process was formulated as different mathematical models.

When an outage occurs, the system operator will follow, adjust, and update the preventive schedule (e.g., RC and MER allocation) based on real-time operating information. Model predictive control (MPC), which can continuously reschedule the restoration process over time, is an appropriate method for post-disaster recovery. In [9][10], MPC was employed to adjust the network topology, distributed energy resource schedule, or the microgrid operation mode based on the latest data.

Based on these analyses, it is known that accurately predicting the power outage, identifying vulnerable areas, and evaluating the unserved load in a disturbance are critical for the whole restoration process. In this context, this paper mainly focuses on the preventive stage to evaluate the possible damage caused by extreme weather to aid the system operator. First, the outputs of an existing outage prediction model (OPM) tool are used to identify a set of vulnerable lines in an extreme weather event. Then, all possible faulted line scenarios are enumerated, and the corresponding nodal unserved load profiles are obtained by running a three-phase restoration model. Finally, the nodal unserved load profiles are clustered into multiple representative profiles that can provide concise and direct information about the unserved load to the system operator. These profiles can be further used to seek support from neighboring utilities in

This work was authored in part by the National Renewable Energy Laboratory, operated by Alliance for Sustainable Energy, LLC, for the U.S. Department of Energy (DOE) under Contract No. DE-AC36-08GO28308. Funding provided by U.S. Department of Energy Office of Energy Efficiency and Renewable Energy Solar Energy Technologies Office Award Number DE-EE0010422. The views expressed in the article do not necessarily represent the views of the DOE or the U.S. Government. The U.S. Government retains and the publisher, by accepting the article for publication, acknowledges that the U.S. Government retains a nonexclusive, paid-up, irrevocable, worldwide license to publish or reproduce the published form of this work, or allow others to do so, for U.S. Government purposes.

advance and guide MER investment which will be the focus of the future work. The contributions of this work are summarized as follows:

- An optimal three-phase distribution system restoration model is established considering the allocation of MERs and the schedule of RCs.
- A novel scenario clustering algorithm is proposed to reduce the scenario scale based on the accumulated nodal unserved load.
- The integration of MERs and RCs has been proved to significantly reduce the unserved load, and the representative scenarios can effectively preserve information of original scenarios.

II. Outage Prediction Model

The OPM tool developed by the Eversource Energy Center at the University of Connecticut can predict outages associated with extreme weather events in the northeastern United States [11]. This tool is based on meteorological, statistical, and ML techniques. The tool includes two types of inputs: weather and environment data and power grid data. Weather and environment data consist of land cover, vegetation, and historical weather events, such as wind speed, precipitation, temperature, and humidity. Power grid data includes electric infrastructure, network topology, historical outages, failed equipment, etc. The core of the OPM tool is five ML models. After the OPM is trained, it can predict the possible outages for the system operator to develop preparedness measures.

However, to utilize OPM outputs for resilience enhancement, system operators need more accurate prediction of outage types and devices/assets that are most likely to suffer from failures. Therefore, the OPM outputs need to be processed to extract information that can be used to direct preventative measures. In this paper, we take OPM results as inputs and introduce scenario enumeration and scenario reduction modules to obtain potential device failure scenarios, which will be further integrated into optimization models to allocate resources to maximize distribution system resilience. The workflow is shown in Fig. 1.

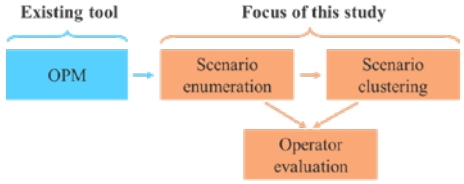

Fig. 1. Workflow of this paper.

III. Three-Phase Distribution System Restoration Model

This section presents an optimal three-phase distribution system restoration model, including power flow modeling, stationary distributed generation modeling, MER allocation, and RC scheduling.

A. Objective Function

The objective minimizes the expected energy not served (EENS) during the system restoration, which is expressed in (1).

$$min.\ \sum_{t\in\Omega_T}\Delta t\sum_{i\in\Omega_B}\sum_{\phi\in\Omega_\phi}\omega_p P_{i,\phi,t}^{eens}+\omega_q Q_{i,\phi,t}^{eens} \quad (1)$$

where $P_{i,\phi,t}^{eens}$ and $Q_{i,\phi,t}^{eens}$ represent the active and reactive unserved load at bus i at phase ϕ at time t, respectively; Δt refers to the scheduling time slot.

B. Three-Phase Power Flow

The distribution system operation constraints are given by (2)-(10). Note that $\forall i \in \Omega_B, \forall \phi \in \Omega_\phi, \forall t \in \Omega_T, \forall ij \in \Omega_L$ after each constraint are neglected for simplicity:

$$P_{i,\phi,t}^{MT}+P_{i,\phi,t}^{PV}+P_{i,\phi,t}^{MER}-P_{i,\phi,t}^{D}+P_{i,\phi,t}^{eens}= \sum_{k\in\delta(i)}P_{ik,\phi,t}-\sum_{j\in\pi(i)}P_{ji,\phi,t} \quad (2)$$

$$Q_{i,\phi,t}^{MT}+Q_{i,\phi,t}^{PV}-Q_{i,\phi,t}^{D}+Q_{i,\phi,t}^{eens}= \sum_{k\in\delta(i)}Q_{ik,\phi,t}-\sum_{j\in\pi(i)}Q_{ji,\phi,t} \quad (3)$$

$$0\le P_{i,\phi,t}^{eens}\le P_{i,\phi,t}^{D} \quad (4)$$

$$0\le Q_{i,\phi,t}^{eens}\le Q_{i,\phi,t}^{D} \quad (5)$$

$$-\left(S_{ij,\phi,t}^{max}\right)^2\cdot\gamma_{ij,t}\le {P_{ij,\phi,t}}^2+{Q_{ij,\phi,t}}^2\le\left(S_{ij,\phi,t}^{max}\right)^2\cdot\gamma_{ij,t} \quad (6)$$

$$v_{j,\phi,t}=v_{i,\phi,t}-\Delta v_{ij,\phi,t}-2\left(\tilde{\boldsymbol{r}}_{ij,\phi}\boldsymbol{P}_{ij,t}+\tilde{\boldsymbol{x}}_{ij,\phi}\boldsymbol{Q}_{ij,t}\right) \quad (7)$$

$$\left(V_{i,\phi,t}^{min}\right)^2\le v_{i,\phi,t}\le\left(V_{i,\phi,t}^{max}\right)^2 \quad (8)$$

$$-M\left(1-\gamma_{ij,t}\right)\le\Delta v_{ij,\phi,t}\le M\left(1-\gamma_{ij,t}\right) \quad (9)$$

$$\gamma_{ij,t}\in\{0,1\} \quad (10)$$

$$\boldsymbol{P}_{ij,t}=\left[P_{ij,\phi^a,t},P_{ij,\phi^b,t},P_{ij,\phi^c,t}\right]^{\mathrm{T}} \quad (11)$$

$$\boldsymbol{Q}_{ij,t}=\left[Q_{ij,\phi^a,t},Q_{ij,\phi^b,t},Q_{ij,\phi^c,t}\right]^{\mathrm{T}} \quad (12)$$

where (2)-(3) represent the active and reactive power balance constraints, in which $P_{i,\phi,t}^{MT}$, $P_{i,\phi,t}^{PV}$ and $P_{i,\phi,t}^{MER}$ represent the active power output of microturbines (MTs), photovoltaic (PV) units and MERs respectively, $P_{i,\phi,t}^{D}$ is the electricity load; (4)-(5) limit the unserved load so that it cannot exceed the original load; (6) is the distribution line congestion constraint, which can be approximated by three piecewise linear constraints [3], $P_{ij,\phi,t}$ and $Q_{ij,\phi,t}$ represent the active and reactive power flow of line ij; (7) is the voltage drop expression neglecting power losses, the detailed derivation can be found in [9], a slack variable $\Delta v_{ij,\phi,t}$ is introduced to relax (7) if line ij is in fault; in (9), $\Delta v_{ij,\phi,t}$ is forced to be zero if line ij has been restored, $\Delta v_{ij,\phi,t}$ becomes an unbounded variable when line ij is in fault since node i and node j is disconnected, the large value of M ensures a broad range for $\Delta v_{ij,\phi,t}$, rendering $\Delta v_{ij,\phi,t}$ unbounded to some extent; $\gamma_{ij,t}$ is a binary variable indicating the status of distribution line ij at time t, where 1 refers to normal, and 0 refers to a fault; (11) and (12) represent the vectors of the single-phase components which are donated by the superscripts a, b and c.

C. Stationary Distributed Generator Operation Constraints

Stationary distributed generators include PV units and MTs. Their power output constraints are shown in (13)-(17).

$$0\le P_{i,\phi,t}^{PV}\le P_{i,\phi,t}^{PV,fore} \quad (13)$$

$$-P_{i,\phi,t}^{PV}\tan(\arccos\alpha_i)\le Q_{i,\phi,t}^{PV}\le P_{i,\phi,t}^{PV}\tan(\arccos\alpha_i) \quad (14)$$

$$-\left(S_{\square}^{PV,max}\right)^2\le {P_{i,\phi,t}^{PV}}^2+{Q_{i,\phi,t}^{PV}}^2\le\left(S_{\square}^{PV,max}\right)^2 \quad (15)$$

$$P_{i,\phi}^{MT,min}\le P_{i,\phi,t}^{MT}\le P_{i,\phi}^{MT,max} \quad (16)$$

$$0\le Q_{i,\phi,t}^{MT}\le P_{i,\phi,t}^{MT}\tan(\arccos\alpha_i) \quad (17)$$

where (15) ensures PV's output will not exceed its nameplate capacity, it's approximated by three piecewise linear constraints [3]; α is the power factor [12], it should be noted that α cannot be an arbitrary value for MTs since synchronous machine cannot operate at all power factors. Therefore, α should be set as a reasonable value.

D. Mobile Energy Resource Allocation

MERs include MDGs and MBESSs in this study. The power output constraints of MDG are similar to those of MTs, and power constraints of MBESSs can be found in [12]. They are neglected here for simplicity. MERs can travel between different locations to provide temporary power supply. The moving process can be represented by the following constraints [8]:

$$\sum_{i\in \mathrm{N_m}} y_{m,i,t} \le 1,\ \forall m \in \Omega_M \tag{18}$$

$$\sum_{m\in\Omega_M} y_{m,i,t} \le Cap_i,\ \forall i \in \cup_{m\in\Omega_M} \mathrm{N_m} \tag{19}$$

$$z_{m,t} = 1 - \sum_{i\in \mathrm{N_m}} y_{m,i,t},\ \forall m \in \Omega_M \tag{20}$$

$$y_{m,i,t+\tau} + y_{m,j,t} \le 1, \forall m \in \Omega_M, \forall i,j \in \mathrm{N_m},$$
$$\forall \tau \le t^{tr}_{m,i,j},\ \forall t+\tau \le |\Omega_T| \tag{21}$$

where $\mathrm{N_m}$ represents the grid connection node set that MER m can access; $y_{m,i,t}$ represents that MER m connects to node i at time t; $z_{m,t}$ represents that MER m is moving from one location to another; (18) enforces that MER m can only connect to at most one node at t; (19) means at most Cap_i MERs can connect node i; (20) indicates that MER m is either connecting to a node or moving; and (21) is the transportation time from node j to node i.

E. Repair Crew Scheduling

The routing schedule optimization of MERs and RCs shares many similarities, but it also has some critical differences. 1) The faulted or damaged equipment is repaired by only one RC only once. An MER can connect to the grid at the same node more than once. 2) The duration to repair the equipment can be assumed to be a fixed number according to experience, whereas the duration of a MER connecting to a node is variable.

In addition to the routing constraints (18)-(21), the following constraints should also be satisfied for the RC scheduling [8]:

$$\gamma_{ij,t} \le \frac{\sum_{\tau=1}^{t} y_{m,ij,t}}{t^{rc}_{m,ij}}, \forall m \in \Omega_{RC}, \forall ij \in \Omega_F \tag{22}$$

$$\gamma_{ij,t} \le \gamma_{ij,t+1}, \forall ij \in \Omega_F \tag{23}$$

where Ω_F is the faulted line set, $t^{rc}_{m,ij}$ refers to the repair time of faulted line ij; (22) restricts the repair time; and (23) indicates that the line remains normal after being repaired.

IV. K-Means-Based Scenario Clustering

Given the vulnerable distribution lines, the possible faulted line scenarios can be enumerated. The scenario number can be up to the hundreds or even thousands. It will be challenging for the system operator to investigate and make schedules for each scenario; therefore, the scenario clustering strategy is ideal for reducing all possible scenarios to some representative scenarios.

In this study, each scenario represents the faulted lines that are expressed by binary variables, and it is not easy to directly find similar characteristics. Different from the traditional scenario clustering strategies that are based on a scenario's self-characteristics (e.g., similar PV/load profiles), a novel scenario clustering strategy is proposed.

Based on the faulted lines, the unserved load at different locations can be estimated, and this information is also what the system operator cares about most. Because different faulted lines can lead to similar unserved load profiles, the accumulated nodal unserved load profile over time can work as the characteristic for the scenario clustering.

After solving the restoration model for every scenario independently, its nodal unserved load can be obtained, which is expressed as:

$$\boldsymbol{E}^s = [E_1, E_2, \cdots, E_{|\Omega_B|}] \tag{24}$$

where E_i is the accumulated unserved load of bus i, which is the sum of the unserved load over time:

$$E_i = \Delta t \sum_{t\in\Omega_T} \sum_{\phi\in\Omega_\Phi} P^{eens}_{i,\phi,t} \tag{25}$$

Two scenarios with different faulted lines but similar accumulated nodal unserved load profiles are illustrated in Fig. 2. Because these two scenarios have similar nodal unserved load and profiles, it is reasonable to consider them as one kind of scenario.

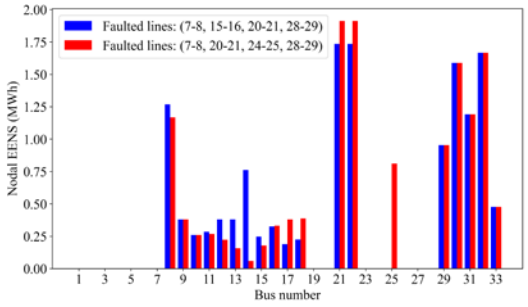

Fig. 2. Nodal unserved load profiles of two scenarios.

K-means is a commonly used method to partition a series of observations into k clusters. In this study, k-means is used to cluster all possible unserved load profiles into multiple representative profiles. The detailed procedure is shown in Algorithm 1.

Algorithm 1: Scenario Clustering

1. Scenario generation: Enumerate all possible faulted line scenarios based on the OPM outputs.

2. Initialization: For each $s \in \Omega_S$, solve (1)-(23), and calculate $\boldsymbol{E}^s$ via (24)-(25).

3. *K*-means clustering:

3.1. Select a proper k.

3.2. Run the k-means algorithm. The algorithm aims to minimize the within-cluster sum of squares (WCSS):

$$WCSS \in argmin \sum_{i=1}^{k} \sum_{s\in\Omega_{Si}} \|\boldsymbol{E}^s - \boldsymbol{\mu}_i\|^2$$

where $\boldsymbol{\mu}_i$ is the centroid of cluster i.

3.3. Update the probability of clusters.

$$p(i) = \sum_{s\in\Omega_{Si}} p(s)$$

V. Case Studies

The proposed model is tested on a modified three-phase IEEE 33-bus distribution system. Simulations are performed on a laptop with Intel Core i7-1165G7 2.80 GHz CPU, and 16 GB RAM. The coding work is performed in Visual Studio Code,

utilizing Python 3.9.7 as the programming language and Gurobi 9.5.0 [13] as the optimization solver.

A. Modified Three-Phase IEEE 33-Bus System

In this study, the standard single-phase IEEE 33-bus system [14] is extended to a three-phase system for simulation. The single-phase diagram is shown in Fig. 3 for simplicity. One stationary PV unit, one MT, and one shunt capacitor are installed in the system. It is set $\omega_p = 0.9$ and $\omega_q = 0.1$. Because in an extreme event, it is more important to provide active power for consumers, especially when voltage level is maintinaed in an acceptable range. Power factor α is set to 0.95 for both PV, MT, and MDG units. An 18-node transportation system is designed to evaluate the proposed methodology. It has 10 MBESS connection nodes, 11 MDG connection nodes, and 3 coupled nodes for both the MBESS and MDG. Two RCs, one MBESS, and two MDGs are assumed in the system.

Based on the OPM outputs, 9 vulnerable lines are identified: {3-4, 7-8, 9-10, 12-13, 15-16, 20-21, 24-25, 28-29, 31-32}, and assume 4 of them will be in a fault; thus, there will be 126 scenarios by enumeration. The outage start time is 5:00 AM.

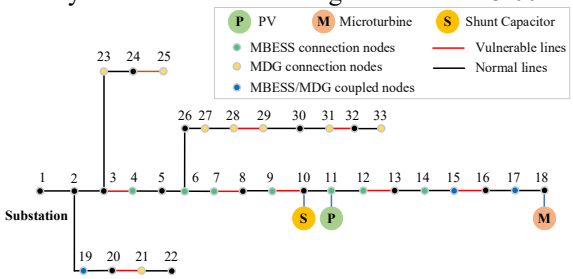

Fig. 3. Diagram of the single-phase IEEE 33-bus system.

B. Scenario Clustering Without MERs

K-means algorithm is performed by using the "sklearn" library [15]. The elbow method is used to determine the number of clusters. It is found an elbow appears between k = 15 and k =25, which means that when k > 25, the WCSS slowly decreases; therefore, we select k = 25 as the number of clusters.

After the scenario clustering, the 126 scenarios are clustered into 25 scenarios. To show the clustering performance, the nodal EENS profiles before and after the *k*-means clustering of Cluster 8 are illustrated in Fig. 4. The centroid can represent the original unserved load profiles. The vulnerable areas in this cluster can also be identified: buses 7, 8, 13, 14, 25, 30, 31, and 32. To illustrate the overall discrepancy between the centroid and cluster members, the average root mean squared error (RAMSE) of all clusters is calculated. RAMSE is 6.11% of average total EENS which is small, indicating the centroid can well preserve the information of cluster members.

The quantitative comparison between the original and clustered scenarios is shown in Table I. The total number of EENS is divided into six ranges with each range having a 5-MWh interval. Each range represents a damage level indicating the unserved load caused by the extreme weather event.

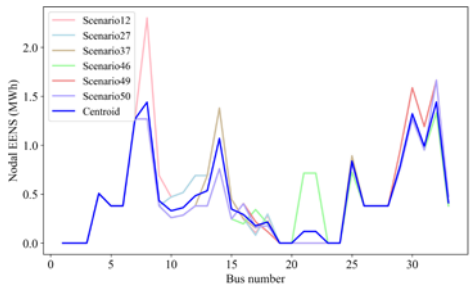

Fig. 4. Original scenarios and the centroid of Cluster 8.

This table shows that the probability of the unserved load between 5 MWh and 25 MWh can reach 96.82%. This result can give the system operator quantitative information about the damage levels. Another finding is that the unserved load probability obtained by the clustered scenarios is similar to that of the original scenarios. This means that the system operator can focus on a limited number of scenarios to evaluate the damage level instead of analyzing all possible scenarios, which improves efficiency. This also verifies the effectiveness of the proposed scenario clustering strategy.

TABLE I. COMPARISON OF THE SCENARIOS WITHOUT MERS.

Total EENS (MWh)	Unserved load ratio (%)	Original probability (%)	Clustered probability (%)
0 - 5	0 - 4.77	1.59	0
5 - 10	4.77 - 9.55	20.63	20.63
10 - 15	9.55 - 14.32	27.78	29.36
15 - 20	14.32 - 19.09	36.51	40.86
20 - 25	19.09 - 23.87	11.90	9.14
25 - 30	23.87 - 28.64	1.59	0

C. Scenario Clustering with MERs

In this subsection, MERs are integrated into the restoration model to show the resilience improvement. To demonstrate the effectiveness of MERs, a specific scenario is selected as an example in which the faulted lines are 3-4, 7-8, 12-13, and 15-16. The RC schedule and MER allocation are shown in Fig. 5 and Fig. 6, respectively. In Fig. 5, RC 1 takes 4 hours to repair line 3-4, and then it takes 2 hours to drive to line 12-13 for repairs. At t = 18, all faulted lines are repaired, and the distribution system returns to normal operation.

In Fig. 6, the MERs move between different locations to provide emergency power. The bus number is shown in the box. This process considers the faulted line status. For example, when one fault is cleared and the corresponding area is recovered, the MDGs will move to another faulted area, and the MBESS will move to the nearest normal location for charging and move to the faulted area for discharging. The MERs will return to the depot when all the faults are cleared.

Table II shows the quantitative results considering MERs. It can be observed that the probabilities calculated by the original and clustered scenarios are also very close, which further validates that the clustered scenarios can well represent the original scenarios. Additionally, the unserved load is significantly reduced compared with Table I. For example, in 97.62% of the scenarios, the unserved load is contained within 15 MWh, contrasting with only 50% of the scenarios as presented in Table I. In Table II, none of the scenarios does the unserved load exceed 20 MWh, whereas this figure stands at 13.49% in Table I. Additionally, the average total EENS of all outage scenarios without MERs is 14.62 MWh. This figure

drops to 7.46 MWh with the deployment of MERs, marking a reduction of 48.97%.

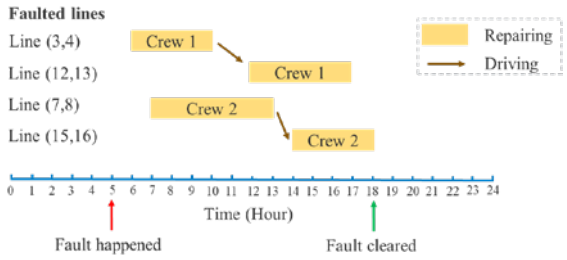

Fig. 5. RC schedule.

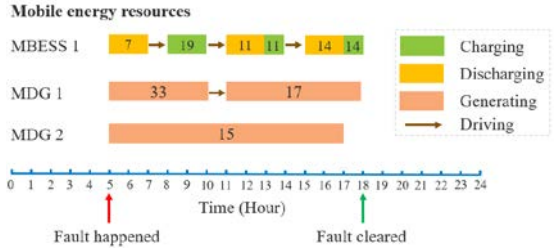

Fig. 6. MER allocation.

TABLE II. COMPARISON OF THE SCENARIOS WITH MERS.

Total EENS (MWh)	Unserved load ratio (%)	Original probability (%)	Clustered probability (%)
0 - 5	0 - 4.77	37.30	37.30
5 - 10	4.77 - 9.55	25.40	20.63
10 - 15	9.55 - 14.32	34.92	40.48
15 - 20	14.32 - 19.09	2.38	1.59
20 - 25	19.09 - 23.87	0	0
25 - 30	23.87 - 28.64	0	0

D. Financial and Voltage Comparison Without/With MERs

By considering MDG's fuel cost, MBESS's energy loss between charging and discharging, and MDG and MBESS's transportation fuel cost, MER's operational cost during the outage is estimated in [$1212.72, $2393.88]. Consumer financial loss is estimated to be $49849.32 without MERs and $25282.92 with MERs [16]. The saving is $24566.40 which is far more than the maximum operational cost of $2393.88 by employing MERs. Based on this analysis, the financial benefit of using MERs during outages is believed to be significant.

The example faulted line scenario in Subsection V.C. is used here. The three-phase voltage at node 33 without and with MERs are shown in Fig. 7. In (a), at t = 5, the four lines are in fault, node 33 disconnects from the main grid and there is no MER. Therefore, the voltage drops to 0. From Fig. 6, line 3-4 is repaired at t = 10, then node 33 recovers the connection with the main grid and its voltage has a profile. In (b), between t = 5 and t = 10, an MDG connects to node 33. Therefore, the voltage at node 33 is maintained in the acceptable voltage range.

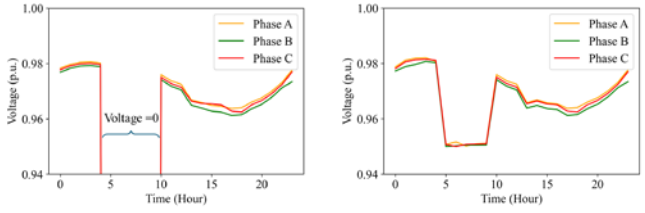

(a) Without MERs (b) With MERs

Fig. 7. Three-phase voltage at node 33.

VI. CONCLUSIONS AND FUTURE WORK

Accurate outage estimation enables system operators to better understand the possible damage caused by an extreme weather event. Given the vulnerable lines and their numerous combinations, this paper proposes a scenario clustering strategy to reduce the number of nodal unserved load profiles. The numerical simulation verifies that the representative scenarios can maintain the characteristics of the original scenarios. These representative unserved load profiles provide the system operator with straightforward information regarding the unserved load and vulnerable areas. The improvement of the MER integration in the restoration process is also quantitively evaluated.

Future work will focus on investigating the applications of preventive outage analysis: 1) Determining how to collaborate with neighboring utilities to best allocate the available MERs; 2) Utilities can optimally allocate its budget to bolster resilience through various measures based on the representative scenarios.

REFERENCES

[1] Z. Bie, Y. Lin, G. Li, and F. Li, "Battling the extreme: A study on the power system resilience," *Proc. IEEE*, vol. 105, no. 7, pp. 1253-1266, July 2017.

[2] National Centers for Environmental Information. Accessed: Oct. 11, 2023. [Online] Available: https://www.ncei.noaa.gov/access/billions/time-series.

[3] Q. Shi, F. Li, T. Kuruganti, M. M. Olama, J. Dong, X. Wang *et al.*, "Resilience-oriented DG siting and sizing considering stochastic scenario reduction," *IEEE Trans. Power Syst.*, vol. 36, no. 4, pp. 3715-3727, July 2021.

[4] M. Mohammadian, F. Aminifar, N. Amjady, and M. Shahidehpour, "Data-driven classifier for extreme outage prediction based on Bayes decision theory," *IEEE Trans. Power Syst.*, vol. 36, no. 6, pp. 4906-4914, Nov. 2021.

[5] Y. Yao, W. Liu, R. Jain, S. Madasthu, B. Chowdhury, and R. Cox, "Outage forecast-based preventative scheduling model for distribution system resilience enhancement," *2023 IEEE Power & Energy Society General Meeting (PESGM)*, Orlando, FL, USA, 2023, pp. 1-5

[6] Q. Shi, F. Li, J. Dong, M. M. Olama, X. Wang, C. Winstead *et al.*, "Co-optimization of repairs and dynamic network reconfiguration for improved distribution system resilience," *Appl. Energy*, vol. 318, pp. 119245, 2022.

[7] A. Arif, Z. Wang, J. Wang, and C. Chen, "Power distribution system outage management with co-optimization of repairs, reconfiguration, and DG dispatch," *IEEE Trans. Smart Grid*, vol. 9, no. 5, pp. 4109-4118, Sept. 2018.

[8] S. Lei, C. Chen, Y. Li, and Y. Hou, "Resilient disaster recovery logistics of distribution systems: Co-optimize service restoration with repair crew and mobile power source dispatch," *IEEE Trans. Smart Grid*, vol. 10, no. 6, pp. 6187-6202, Nov. 2019.

[9] W. Liu and F. Ding, "Hierarchical distribution system adaptive restoration with diverse distributed energy resources," *IEEE Trans. Sustain. Energy*, vol. 12, no. 2, pp. 1347-1359, April 2021.

[10] J. Tobajas, F. G. Torres, P. R. Sánchez, J. Vázquez, L. Bellatreche, and E. Nieto, "Resilience-oriented schedule of microgrids with hybrid energy storage system using model predictive control," *Appl. Energy*, vol. 306, pp. 118092, 2022.

[11] D. Cerrai, D. W. Wanik, M. A. E. Bhuiyan, X. Zhang, J. Yang, M. E. B. Frediani *et al.*, "Predicting storm outages through new representations of weather and vegetation," *IEEE Access*, vol. 7, pp. 29639-29654, 2019.

[12] X. Wang, F. Li, J. Dong, M. M. Olama, Q. Zhang *et al*., "Tri-level scheduling model considering residential demand flexibility of aggregated HVACs and EVs under distribution LMP," *IEEE Trans. Smart Grid*, vol. 12, no. 5, pp. 3990–4002, Sep. 2021.
[13] Gurobi Optimization, LLC, "Gurobi Optimizer, Version 9.5.0," 2021. [Online]. Available: https://www.gurobi.com/.
[14] S. H. Dolatabadi, M. Ghorbanian, P. Siano, and N. D. Hatziargyriou, "An enhanced IEEE 33 bus benchmark test system for distribution system studies," *IEEE Trans. Power Syst*., vol. 36, no. 3, pp. 2565-2572, May 2021.
[15] F. Pedregosa, G. Varoquaux, A. Gramfort, V. Michel, B. Thirion, O. Grisel *et al*., "Scikit-learn: Machine learning in Python," *J. Mach. Learn. Res.*, vol. 12, pp. 2825-2830, 2011.
[16] M. J. Sullivan, M. Mercuriov, and J. Schellenberg, "Estimated value of service reliability for electric utility customers in the United States," Lawrence Berkeley Nat. Lab., Berkeley, CA, USA, Tech. Rep. LBNL-2132E, Jun. 2009.